Serrated flow in AZ91 magnesium alloy in tension and compression

Z. Trojanová[1]*, C. H. Cáceres[2], P. Lukáč[1], L. Čížek[3]

[1] *Department of Physics of Materials, Faculty of Mathematics and Physics, Charles University, Ke Karlovu 5, CZ-121 16 Prague 2, Czech Republic*
[2] *ARC Centre of Excellence for Design in Light Metals, Materials Engineering, School of Engineering, The University of Queensland, Brisbane QLD 4072, Australia*
[3] *VŠB-Technical University Ostrava, Tř. 17. listopadu 2172, CZ-708 00 Ostrava, Czech Republic*

Received 31 May 2008, received in revised form 31 July 2008, accepted 31 July 2008

Abstract

AZ91 magnesium alloy exhibits jerky flow when deformed a short time after solution heat treatment and quenching. The occurrence of stress drops and discontinuous plastic deformation has been observed at temperatures in the vicinity of ambient temperature in tension as well as compression. The alloy exhibits some degree of negative strain rate sensitivity. Acoustic emission accompanies the stress drops. It is concluded that successive deformation bands propagate along the gauge length as soon as the material develops gross plastic deformation, regardless of the applied strain rate. The results are discussed in terms of current theories for the Portevin-LeChâtelier effect.

K e y w o r d s: serrated yielding, dislocations, solid solution, diffusion, collective motion of dislocations, acoustic emission

1. Introduction

The Portevin-Le Châtelier (PLC) effect is a consequence of the complex nature of the dislocation dynamics in metals, which depends on many structural parameters such as the type of structure, grain size, texture, concentration and distribution of solute atoms. Plastic deformation occurs inhomogeneously in the microscopic scale due to thermally activated dislocation motion through a field of obstacles. Temporal-spatial deformation inhomogeneities leading to deformation bands are caused by collective dislocation motion. Unstable plastic deformation associated with sharply localised deformation bands of the PLC effect type have been reviewed by Neuhäuser [1]. The PLC effect was observed in fcc, bcc as well as in hcp structures. Three types of PLC bands have been described. The continuously propagating, type A; intermittently propagating, type B, with regular stress drops; and stochastically nucleating, type C. Most papers are devoted to the explanation of B type serrations. A typical case is that of Al-Mg alloys in which the PLC effect is observed at the room temperature [2–9]. Very few papers [8–15] deal with serrated flow in Mg-based alloys. Recently, serrations have been reported in Mg alloys containing two major solutes Y and Nd – Mg-6Y-3Nd-0.4Zr (WE63) at temperatures between 200 and 280 °C [16] and in Mg-(5.0-5.5)Y-(1.5-2.0)Nd(RE)-0.4Zr (WE52) alloy, thermally treated according T6, at temperatures 150–225 °C [17]. The effect has also been reported in solution heat-treated and quenched Mg-9Al-1Zn (AZ91) alloy at room temperature [18, 19]. The onset of the unstable deformation was also studied using acoustic emission (AE) in AZ91 thermally treated alloy [20]. It was shown that PLC bands propagate along the gauge length from nearly zero strain, independently of the applied strain rate.

The objective of this work is to present a more detailed study of serrated flow in AZ91 alloy deformed at various temperatures, in tension and compression.

*Corresponding author: tel.: +420 221911357; fax: +420 221911490; e-mail address: ztrojan@met.mff.cuni.cz

2. Experimental procedure

Commercial magnesium alloy AZ91 (nominal composition in mass %: 9Al-1Zn-0.2Mn-balance Mg) was used for the study. Tensile cylindrical specimens with a reduced section 6 mm in diameter and 25 mm long were machined from the cast ingots. The compression specimens had a diameter of 10 mm and a length of 15 mm. The specimens were given a standard T4 treatment (homogenisation at 413 ℃ for 18 h, then quenching into water of ambient temperature). The deformation tests were performed immediately after the thermal treatment.

Testing was carried out in a universal testing machine INSTRON over the temperature range from 287 K to 373 K at an initial strain rate of the $10^{-4}\,s^{-1}$. A computer-controlled DAKEL-LMS-16 acoustic emission (AE) facility was used to detect and analyse the AE (count rate) during deformation. A miniaturised MST8S transducer (diameter 3 mm, with near-flat response in the frequency band between 100 and 500 kHz) was attached to specimen surface with the help of silicon grease and a spring. A two-threshold level of detection was set for evaluation of the AE signals. The total gain applied to the detector's signal was 94 dB.

3. Experimental results

The stress-strain curve obtained in tension at 293 K is presented in Fig. 1 together with the strain dependence of the work hardening coefficient $\theta = d\sigma/d\varepsilon$. A detailed view of the serrations is presented in the inset. A correlation of the macroscopic serrations on the stress-strain curve with its derivative is well visible. The onset strain of macroscopic serrations in the stress-strain curve is approximately 2 %. The stress drops increase in magnitude with the strain. The stress-strain curve at 323 K is shown in Fig. 2. In this case macroscopic serrations begin at a lower strain, less than 1 %. The serrations develop in this case a very regular pattern, see inset. In Fig. 3 the stress-strain curve observed at 373 K is presented. At this temperature the character of the inhomogeneous deformation changes: the sharp stress drops observed at the lower temperatures are now replaced by a wavy curve. The stress-strain curve obtained at temperature 423 K was smooth, i.e., it exhibited no serrations. Figures 4 through 6 show the equivalent results in compression, for temperatures 287, 323 and 373 K. Unlike for the tensile tests, the serrations in compression were predominantly of a well defined stepwise character. At 373 K a small negative strain was observed preceding the serrations. This negative strain was taken as an indication of a sudden elongation of the specimen during the test.

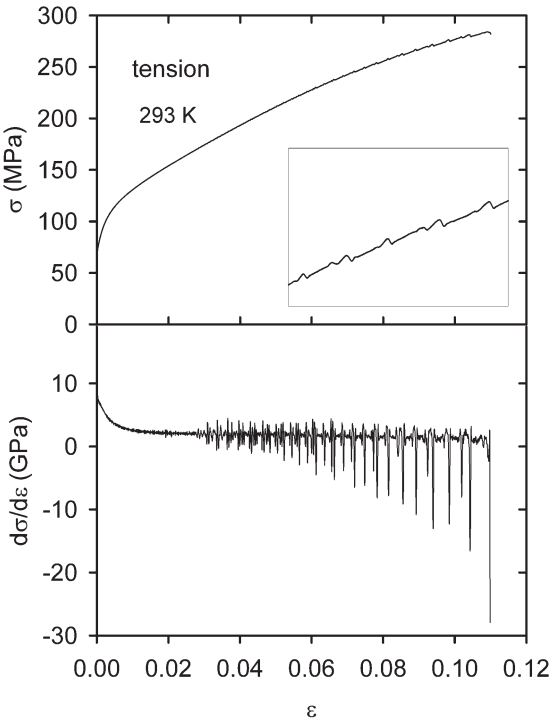

Fig. 1. Stress-strain curve in tension exhibiting serrations visible in the strain dependence of the work hardening coefficient.

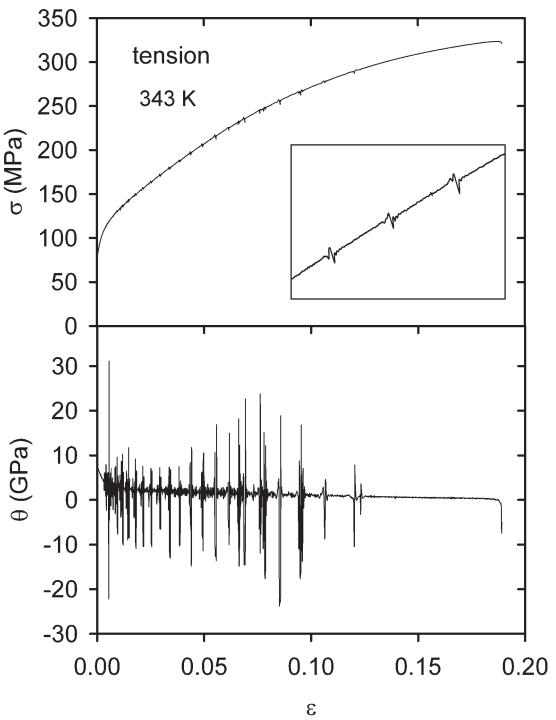

Fig. 2. Stress-strain curve in tension obtained at 343 K together with the stress dependence of work hardening coefficient.

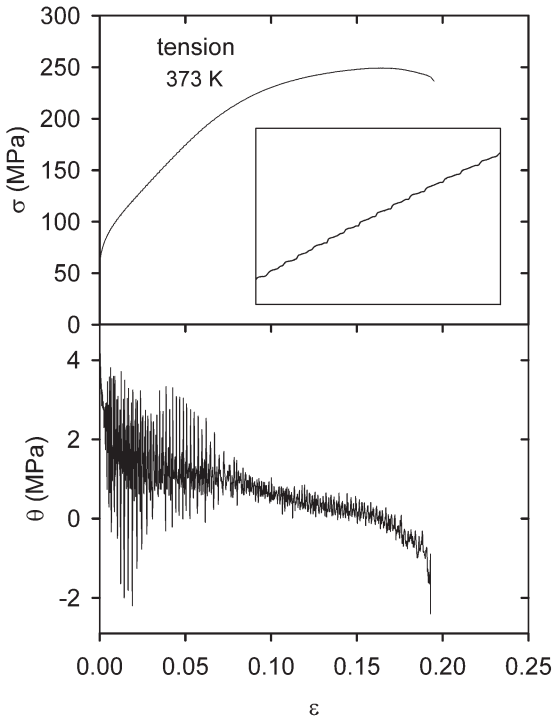

Fig. 3. Stress-strain curve and strain dependence of the work hardening coefficient obtained in tension at 373 K.

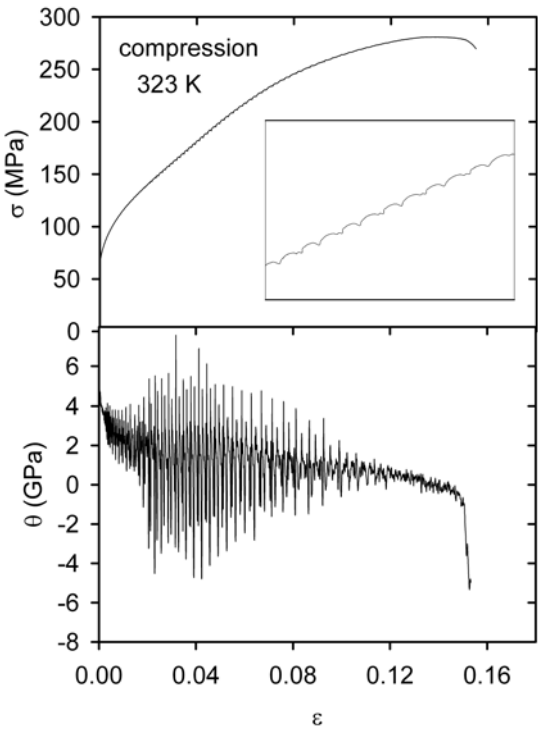

Fig. 5. Stress-strain curve and strain dependence of the work hardening coefficient obtained in compression at 323 K.

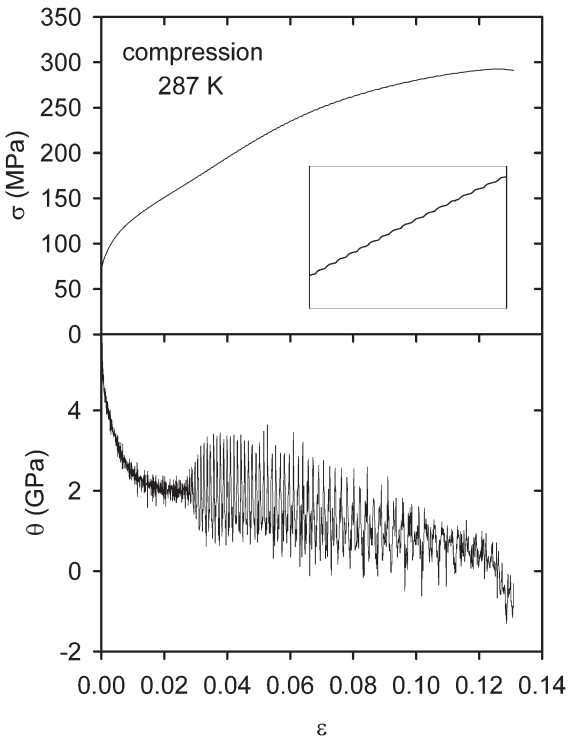

Fig. 4. Stress-strain curve and strain dependence of the work hardening coefficient obtained in compression at 287 K.

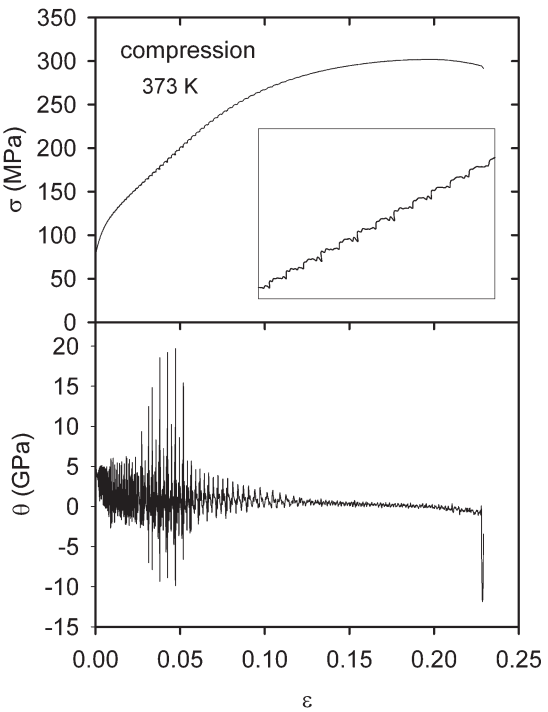

Fig 6. Stress-strain curve and strain dependence of the work hardening coefficient obtained in compression at 373 K.

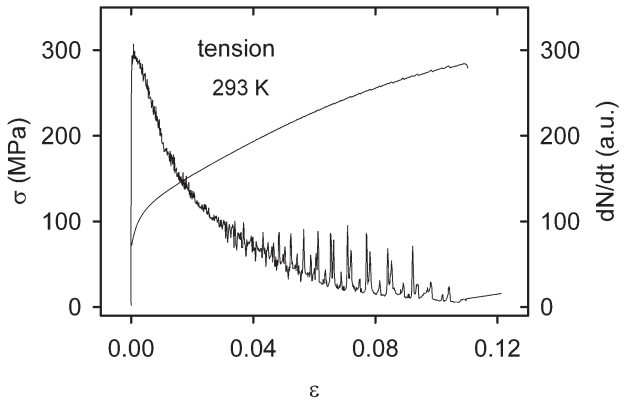

Fig. 7. Stress-strain curve obtained in tension at 293 K together with strain dependence of count rate.

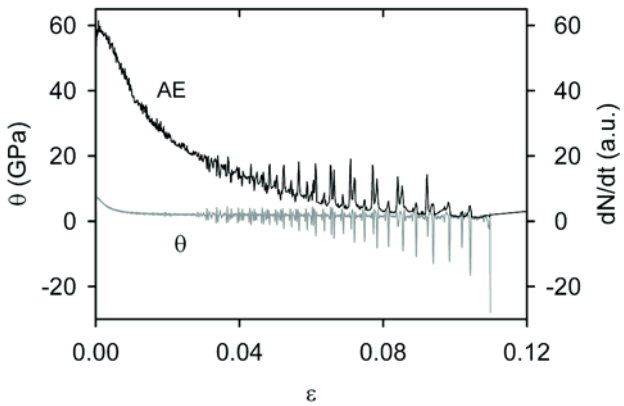

Fig. 8. Strain dependence of AE activity and the work hardening coefficient.

Figure 7 shows the stress-strain curve together with AE measurements obtained for a sample deformed in tension at 293 K. The observed curve exhibits a Lüders phenomenon (small serration at the AE curve) followed by the distinct serrations corresponding to PLC effect. Correspondence of the serrations on the stress-strain curves (or peaks in the strain dependence of the work hardening rate) with the AE peaks is obvious from Fig. 8.

The strain rate dependence of the yield stress for specimens deformed in tension at ambient temperature is shown in Fig. 9. A slightly decreasing dependence could be considered as an indication of the negative strain rate sensitivity typical of the PLC effect. The influence of the strain rate on the magnitude of the stress drops can be seen in Fig. 10, where the stress drops are plotted in the sequence on the stress-strain curves for the two strain rates. Figure 11 compares parts of the stress-strain curves obtained at two different strain rates. Note that the stress-strain axes are common to both curves. The shift is entirely due to the negative strain rate sensitivity.

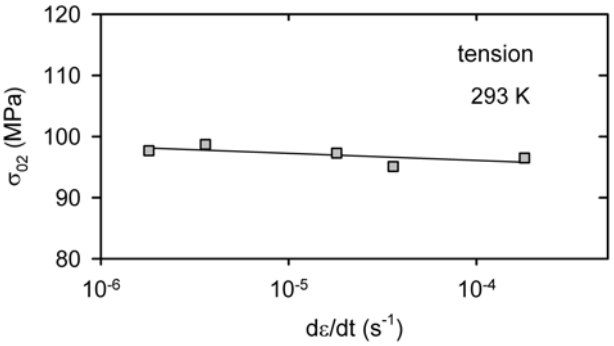

Fig. 9. Strain rate dependence of the yield stress measured in tension at ambient temperature.

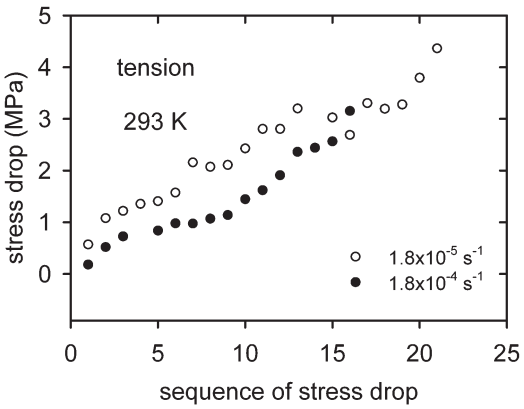

Fig. 10. Strain rate dependence of the starting stress of PLC serrations.

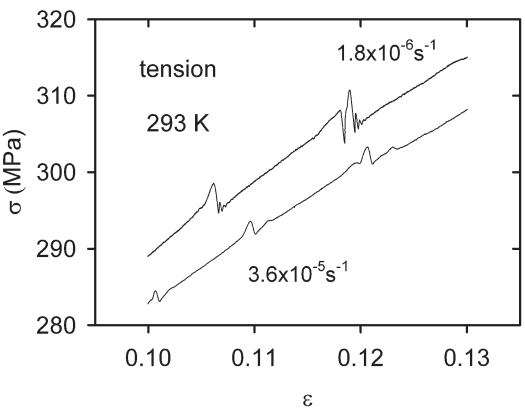

Fig. 11. Sequences of the stress-strain curves obtained for various strain rates. Negative strain rate sensitivity is obvious.

4. Discussion

The main features of serrated flow in AZ91 presented here are very similar to those reported by Chatuverdi et al. [8, 9] for Mg-10%Ag. Chatuverdi et al. used strain-ageing arguments [21, 22] to explain their observations. In principle, the same arguments, i.e., strain ageing effects by Al atoms upon the moving dislocations, could be used to explain serrated flow in the AZ91 alloy. However, there is an important reason to question a straightforward application of a "diffusional" explanation to the present case. It is known from previous experiments [23] in Mg-Al alloys that the binary alloys do not exhibit serrations at room temperature and at the strain rate used in the present study, while the current results also show that serrations develop only when both Al and Zn are present in solid solution. In other words, the availability of a single solute, even at high concentration ([23] as in a Mg-8%Al alloy), is not a sufficient condition for the development of the serrations. On the other hand, there is also possibility that the PLC effect exists at some temperatures different from the ambient temperature, especially in the case of Mg-Zn alloy at a temperature below the room temperature. The PLC effect has been reported in a binary alloy Mg-0.7wt.%Nd [15, 24] and also in the case of ternary WE63 [16] and WE52 [17] alloys.

4.1. Strain hardening

The work hardening of magnesium alloy AZ91 may be easily correlated with the AE activity as shown in Figs. 7 and 8. A rapid increase of AE can be correlated with massive dislocation multiplication, which is an excellent source of AE [25, 26]. Small peaks in the time dependence of AE at the beginning of deformation visible in Fig. 7 can be caused by twinning. In AE, twinning is always accompanied by strong bursts [27]. It is known, that mechanical twinning can play an important role especially in the first stage of deformation of magnesium polycrystals [27–29]. The main twinning system is $\{10\bar{1}2\}\langle 10\bar{1}0\rangle$, the activation of which causes a misorientation of 86.3° between across any twinning interface. Thompson and Millard [28] suggested the following dislocation reaction for twinning:

$$[0001] \rightarrow \alpha\,[10\bar{1}1] + [\bar{1}010]\,, \qquad (1)$$

where α is a small fraction, ranging from 1/12 up to 1/4. Another mechanism of the twin formation was suggested by Startsev et al. [30] who proposed that a mutual reaction among basal dislocations could result in the formation of twinning dislocations and pyramidal perfect dislocations with the Burgers vector of $[11\bar{2}3]$. As both mechanisms [28, 30] result in the motion of similar dislocations and involve both basal and pyramidal slip systems, it can be concluded that twinning is directly related to the strain hardening. Note that $\langle c\rangle$ dislocations with the Burgers vector [0001] can be formed in reaction between the basal dislocations and pyramidal ones according to [31]

$$\frac{1}{3}\,[11\bar{2}0] + \frac{1}{3}\,[\bar{1}\bar{1}23] \rightarrow [0001]\,, \qquad (2)$$

where the first dislocation moves in the basal plane and the second one in the pyramidal plane. Generally, the formation of obstacles for dislocation motion due to dislocation reactions and twinning may significantly restrict the mean free path of dislocations in the slip plane. Twin boundaries and intersections of forest dislocations are effective barriers to dislocation gliding in the basal plane. The athermal component of the flow stress – the internal stress σ_i – as a function of the applied stress σ for AZ91 alloy deformed at room temperature was studied using stress relaxation tests and minimum creep rate method [32]. It was estimated that the internal stress represents a substantial component of the flow stress. Longer-range obstacles are important for the plastic flow of AZ91 alloy.

4.2. Serrated flow

Current explanations of the phenomenon of jerky flow can be broadly classified into two categories, diffusional and non-diffusional, depending on the details of the interaction between solute and mobile dislocations. Whereas the works by Kubin and Estrin [33], Schwarz [34] and Balík [4] attribute the PLC effect exclusively to dynamic strain ageing phenomena (DSA), Korbel et al. [35–37] explained PLC effect by the built up stress concentrations and their relaxations, while solutes in solution play a dual role: on the one hand, they are ensuring planar glide, and on the other, they help immobilising pile-ups and planar dislocation arrays in the last stages of pile-up formation. High voltage TEM has shown that pile-ups stabilised by solute atoms are not reactivated. Instead, new sources of dislocations become active, expanding the deformation into undeformed regions of the specimen [38, 39]. The occurrence of the DSA effects in the AZ91 alloy [32] observed in stress relaxation and the high level of the internal stress in AZ91 alloy indicate that both DSA effects and dislocation – dislocation interaction are necessary for serrated flow to develop. AE measurements showed that the macroscopic stress drops corresponded to large strain bursts.

A sudden collective breakaway of dislocations piled up in front of dislocation tangles (which can be accompanied by multiplication of released dislocations) and their movement on large distances may be assumed as a main AE source. The idea of pile-up induced dislocation breakaway was supported by TEM observation of Tabata et al. [40], and by observations of slip

band with laser extensometry by Klose et al. [41, 42]. According to [35, 36, 43, 44], glide on the primary slip system results in the formation of stable dislocation pile-ups and associated stress concentrations. Obstacles for dislocation motion can be formed during the prior deformation as has been discussed in the section 4.1.

The difficulty in activating prismatic slip makes the pile-ups formed on the basal planes very stable. The stress concentrations are relaxed by a long-range correlated dislocation motion (cross slip) of a dislocation group in secondary (prismatic) slip system. Such dislocation motion is allowed only for screw dislocations. The edge components of dislocation loops remain in the original slip plane as forest dislocations for dislocation motion in the secondary slip planes. A role of the dislocation forest in hcp structures with the main basal slip was studied by Lavrentev [45]. He showed that an increased forest dislocation density by the prestraining in prismatic slip system led to an unstable plastic deformation in the basal plane.

Similar experiments were conducted by Dosoudil et al. [46]. The authors observed unstable plastic deformation in basal slip of Zn single crystals with increased density of forest dislocations. Simultaneously, AE measurements detected large bursts against the background observed during smooth deformation. These experiments reflect about the relevance of the forest dislocation density. Forest dislocations which density was increased by prior movement of dislocation avalanche are local obstacles for dislocation motion. Cores of dislocations waiting at forest dislocations during thermally activated motion in the slip plane may be occupied by solutes, which are movable due to pipe diffusion. These dislocation groups of waiting dislocations are probably spread over a set of adjacent slip planes, rather than being strictly co-planar. They produce local stress concentrations, which may cause a breakaway of dislocation pile-ups. Measurements on Cu-Al single crystals [41, 42] indicate precursor behaviour of the local strain associated with local stress relaxation prior to the strain avalanche characterised by the stress drop. This type of unstable flow is characteristic of the PLC flow, in which a drop in the load is possible if the strain rate during the formation of the slip bands exceeds the strain rate imposed by the tensile testing machine. A high level of the internal stress in AZ91 alloy allows pass of the deformation bands through the whole sample. As each PLC band runs through the gauge length, the formation of new forest dislocations ensures that the process repeats itself. As the dislocation movement in the slip bands ceases or becomes too slow for the applied strain rate, for instance after a drop in the load or at the end of a PLC band, the applied stress must increase in order to resume deformation. Activation of new sources can only occur by cutting through the forest of dislocations created by secondary slip around slip bands no longer active. The forest dislocations increase the CRSS, but provide little strain hardening [47]. If the activation of a source occurs under conditions of stable planar glide, dislocations can form a dynamic pile-up [48] able to move at increasing speed and decreasing levels of the applied stress because of the development of stress concentration ahead of the moving dislocations. This may spontaneously lead to an avalanche of dislocations that meets the general requirement for unstable tensile flow, since a drop in the load, as observed during the PLC effect, is possible only if the strain rate during the formation of the slip bands exceeds the strain rate imposed by the tensile testing machine [36]. It is interesting to note that the structure instability may be also observed in high temperature plastic flow as reported, for instance, by Boček and Choi [49].

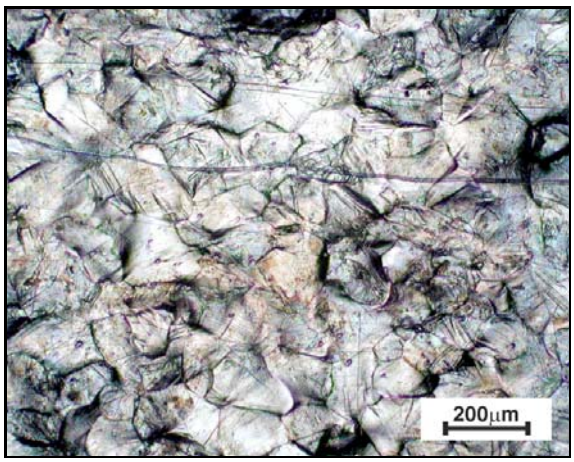

Fig. 12. Optical micrographs showing deformation microstructures of specimen that has been subjected to tensile straining at room temperature.

At low strains, prior to the observation of macroscopic serrations, small bands may traverse the specimen's gauge length at relatively high speed. These bands are very probably of the Lüders type. However, the strain produced by the small bands is small; the strain rate in the band is unable to match the imposed strain rate, and the specimen deforms by a combination of homogeneous and inhomogeneous deformation. Only when the bands develop to the point that the local strain rate is larger than the macroscopically imposed strain rate, the PLC bands concentrate all the strain and the characteristic serrations are observed. At higher strain rates the bands propagate in a smooth fashion, indicating that the strain rate in the band matches the imposed strain rate.

The optical micrograph of Fig. 12 shows slip traces in a specimen subjected to plastic tensile elongation at room temperature. It is common to observe traces of slip bands and deformation twins. The wavy character

of the scratch made before the deformation reflects the slip transfer among the grains.

Comparing these experimental results with binary and ternary Mg-Y-Nd alloys it seems to be probable that only one type of solute atoms is responsible for the PLC effect. Separation of solutes is very probably given by temperature. In order to answer this question, further experiments using binary alloys at different temperatures and strain rates should be performed.

4.3. Compression tests

As it can be seen from Figs. 4–6, the PLC effect has a different character in compression comparing with the observations in tension. The wavy character of the serrations observed at 287 and 323 K changed into stepwise at 373 K. As it can be seen from the inset, the stress is nearly constant within the small strain (time) interval, or slightly decreasing following the rapid stress increase, while the strain exhibits a slightly negative trend prior to the steps. This step in the stress is only possible when the sample is suddenly elongated under the applied compression stresses. Li [50] and Vianco and Li [51] observed negative creep, defined as a contraction of the sample length on the application of the tensile stress. Similarly Trojanová and Lukáč reported negative stress relaxation observed on Zn-Al single crystals [52]. The sample was deformed in tension then the machine was stopped and the sample allowed relaxing. After the first decrease of the stress with the time, the stress increased up to the level at which the stress relaxation started. After reaching this stress level, the stress stepwise decreased following again a slow increase of the stress. This process repeated several times in the time interval of three hours when the stress relaxation was interrupted. The observed stress increase can be explained only as the shortening of the sample under the tension stress. However, it is difficult to understand why the tensile stress can enhance the negative creep or the stress relaxation and on the other hand the compression stresses the elongation of the sample. Dislocation motion in the opposite direction may be invoked by the internal stress fields which are for the dislocation motion more important.

5. Summary and conclusions

Experimental data on the PLC effect in AZ91 magnesium alloy are presented. Samples were deformed in tension as well as in compression over the temperature range from 287 to 373 K. All stress-strain curves exhibited the serrations. Serrations in the stress-strain curves of samples deformed in tension and compression begin at low strains. There is a good correlation between serrations and peaks in the strain dependence of the work hardening rate. Character of serrations in the stress-strain curves of samples deformed in compression is different in comparison with the tension tests. The stepwise character of curves (especially at 373 K) indicates a sudden elongation of the sample during the compression test. Acoustic emission was used to receive deeper information about details of PLC effect. There is good correspondence of the serrations on the stress-strain curves and the peaks in the strain dependence of the work hardening rate with the AE peaks. Starting out from dynamic strain ageing and non-diffusional explanation of the PLC effect, we tried about convergence both theories in the present paper.

Acknowledgements

The authors dedicate this paper to Prof. Dr. Michael Boček, on the occasion of his 80th birthday. We would like to appreciate his contribution to the field of plastic deformation of hexagonal metals and alloys. The authors acknowledge financial support of the Grant Agency of the Czech Republic under grant 101/06/0768. A part of this work was performed in a frame of the 1M 2560471601 "Eco-centre for Applied Research of Non-ferrous Metals" that is financed by the Ministry of Education, Youth and Sports of the Czech Republic.

References

[1] NEUHÄUSER, H.: In: Dislocation in Solids. Ed.: Nabarro, F. R. N. North Holland, Amsterdam, Vol. *6*, 1983, p. 319.
[2] SPRINGER, F.—NORTMANN, A.—SCHWINK, Ch.: Phys. Stat. Sol. (a), *170*, 1998, p. 63.
[3] BALÍK, J.—LUKÁČ, P.—KUBIN, L. P.: Scripta Mater., *42*, 2000, p. 465.
[4] BALÍK, J.: Mater. Sci. Eng. A, *316*, 2001, p. 102.
[5] ZIEGENBEIN, A.—HÄHNER, P.—NEUHÄUSER, H.: Mater. Sci. Eng. A, *309–310*, 2001, p. 336.
[6] LEBYODKIN, M.—FRESSENGEAS, C.—ANATHAKRISHNA, G.—KUBIN, L. P.: Mater. Sci. Eng. A, *319-321*, 2001, p. 170.
[7] NEUHÄUSER, H.—LESSING, J.—SCHÜLKE, M.: J. Mech. Behav. Mater., *2*, 1990, p. 231.
[8] CHATUVERDI, M.—LLOYD, D. J.—TANGRI, K.: Metal. Sci. J., *6*, 1972, p. 16.
[9] CHATUVERDI, M.—LLOYD, J. D.: Phil. Mag., *30*, 1974, p. 1199.
[10] COULING, S. L.: Acta Metall., *7*, 1959, p. 133.
[11] KENT, K. G.—KELLY, A.: J. Inst. Met., *5*, 1864, p. 536.
[12] MIKULOWSKI, B.—KORBEL, A.: Scripta Metall., *16*, 1982, p. 1219.
[13] TOAZ, M. W.—RIPLING, E. J.: J. Inst. Metals, *85*, 1956–1957, p. 137.
[14] ROBINSON, M. J.: Int. Mater. Rev., *39*, 1994, p. 217.
[15] GÄRTNEROVÁ, V.—TROJANOVÁ, Z.—JÄGER, A.—PALČEK, P.: J. Alloys Comp., *378*, 2004, p. 180.

[16] VON BUCH, F.—MORDIKE, B. L.: In: Magnesium Alloys and Technology. Ed.: Kainer, K. U. Weinheim, WILEY-VCH 2003, p. 110.
[17] ZHU, S. M.—NIE, J. F.: Scripta Mater., *50*, 2004, p. 51.
[18] CÁCERES, C. H.—GRIFFITHS, J. R.—DAVIDSON, C. J.—NEWTON, C. L.: Mater. Sci. Eng. A, *325*, 2002, p. 344.
[19] CORBY, C.—CÁCERES, C. H.—LUKÁČ, P.: Mater. Sci. Eng. A, *387–389*, 2004, p. 22.
[20] TROJANOVÁ, Z.—CÁCERES, C. H.: Scripta Mater., *56*, 2007, p. 793.
[21] COTTRELL, A. H.: Phil. Mag., *44*, 1953, p. 829.
[22] McCORMICK, P. G.: Acta Metall., *29*, 1972, p. 1553.
[23] CÁCERES, C. H.—ROVERA, D. M.: J. Light Metals, *1*, 2001, p. 151.
[24] TROJANOVÁ, Z.—GÄRTNEROVÁ, V.—PADALKA, O.: Kovove Mater., *42*, 2004, p. 206.
[25] HEIPLE, C. R.—CARPENTER, S. H.: J. Acoust. Emission, *6*, 1987. p. 177.
[26] HANUŠ, A.—LICHÝ, P.—KOZELSKÝ, P.—ČÍŽEK, L.—CRHA, J.: Acta Metall. Slovaca, *12*, 2006, p. 443.
[27] DOBROŇ, P.—BOHLEN, J.—CHMELÍK, F.—LUKÁČ, P.—LETZIG, D.—KAINER, K. U.: Kovove Mater., *45*, 2007, p. 129.
[28] THOMPSON, N.—MILLARD, D. J.: Phil. Mag., *43*, 1952, p. 422.
[29] LUKÁČ, P.—KOCICH, R.—GREGER, M.—PADALKA, O.—SZÁRAZ, Z.: Kovove Mater., *45*, 2007, p. 115.
[30] STARTSEV, V. I.—SOLDATOV, V. P.—BRODSKYI, M. M.: Phys. Stat. Sol. (a), 1966, p. 863.
[31] BALÍK, J.—LUKÁČ, P.—BOHLEN, J.—KAINER, K. U.: Kovove Mater., *45*, 2007, p. 135.
[32] TROJANOVÁ, Z.—LUKÁČ, P.—MILIČKA, K.—SZÁRAZ, Z.: Mater. Sci. Eng. A, *387–389*, 2004, p. 80.
[33] KUBIN, P. L.—ESTRIN, Y.: Scripta Metall. Mater., *29*, 1993, p. 1147.
[34] SCHWARZ, R. B. In: Proc. of ICSMA 7. Eds.: McQueen, H. et al. Toronto, Pergamon Press 1985, p. 343.
[35] KORBEL, A.—ZASADZIŃSKI, J.—SIEŁUCKA, Z.: Acta Metall., *24*, 1976, p. 919.
[36] KORBEL, A.—DYBIEC, H.: Acta Metall., *29*, 1981, p. 89.
[37] KORBEL, A.: J. Mech. Behav. Mater., *4*, 1992, p. 61.
[38] CLÉMENT, N.—CAILLARD, D.—MARTIN, J. L.: Acta Metall., *32*, 1984, p. 961.
[39] MARTIN, J. L.: R. Phys. Appl., *15*, 1980, p. 853.
[40] TABATA, T.—FUJITA, H.—NAKAJAMA, Y.: Acta Metall., *28*, 1980, p. 795.
[41] KLOSE, F. B.—ZIEGENBEIN, A.—WEIDENMÜLLER, J.—NEUHÄUSER, H.—HÄHNER, P.: Comp. Mater. Science, *26*, 2003, p. 80.
[42] KLOSE, F. B.—ZIEGENBEIN, A.—HAGEMANN, F.—NEUHÄUSER, H.—HÄHNER, P.—ABADDI, M.—ZEGHOUL, A.: Mater. Sci. Eng. A, *269*, 2004, p. 76.
[43] KORBEL, A.—PAWELEK, A.: In: Inter. Conf. on Dislocation Modelling of Physical Systems, Gainesville, FA. Eds.: Ashby, M. F., Bullough, R., Hartley, C. S., Hirth, J. P. Oxford, Pergamon Press 1981, p. 22.
[44] CÁCERES, C. H.—RODRIGUEZ, A. H.: Acta Metall., *35*, 1987, p. 2851.
[45] LAVRENTEV, F. F.: Mater. Sci. Eng. A, *46*, 1980, p. 191.
[46] DOSOUDIL, J.—TROJANOVÁ, Z.—LUKÁČ, P.—CHMELÍK, F.—LAVRENTEV, F. F.: Kovove Mater., *33*, 1995, p. 181.
[47] BASIŃSKI, Z. S.—JACKSON, P. J.: App. Phys. Let., *6*, 1965, p. 148.
[48] NEUHÄUSER, H.—SCHWINK, C.: In: Materials Science and Technology. Eds.: Cahn, R. W., Haasen, P., Kramer, E. J. Vol. 6. Amsterdam, Elsevier 1993, p. 191.
[49] BOČEK, M.—CHOI, H. J.: Mater. Sci. Eng. A, *137*, 1991, p. 111.
[50] LI, J. M. C.: Mater. Sci. Engn., *98*, 1988, p. 465.
[51] VIANKO, P. T.—LI, J. M. C.: Mater. Sci. Engn., *95*, 1987, p. 175.
[52] TROJANOVÁ, Z.—LUKÁČ, P.: Phys. Stat. Sol. (a), *130*, 1992, K35.